Electroencephalographic Source Localization based on Enhanced Empirical Mode Decomposition

Maximiliano Bueno-López, Pablo A. Munoz-Gutierrez, Eduardo Giraldo and Marta Molinas

***Abstract*—In this work, a novel identification method of relevant Intrinsic Mode Functions, obtained from Electroencephalographic signals, by using an entropy criteria is proposed. The idea is to reduce the number of Intrinsic Mode Functions that are necessary for the electroencephalographic source reconstruction. An entropy cost function is applied on the Intrinsic Mode Functions generated by the Empirical Mode Decomposition for automatic IMF selection. The resulting Enhanced Empirical Mode Decomposition is evaluated in simulated and real data bases containing normal and epileptic activity by means of a relative error measure. The proposed approach shows to improve the electroencephalographic source reconstruction specifically for epileptic seizure detection.**

***Index Terms*—Brain mapping, Epileptic seizures, Seizure detection, Empirical-Mode-Decomposition.**

I. Introduction

RICHARD Caton discovered electrical currents in the brain in 1875 and Hans Berger recorded these currents and published the first human Electroencephalogram (EEG) in 1924 [1]. The EEG is used to measure the electrical activity of the brain characterizing its various normal and pathological states. Due to their non-linear and non-stationary nature, these signals are very difficult to analyze in the time -frequency frame. However, important features can be extracted for assisting in the analysis of Alzheimer‘s disease, attention-deficit/hyperactivity disorder (ADHD), autism, autistic spectrum disorder, alcoholism, epileptic seizures, depth of anesthesia, etc. [2], [3], [4]. EEG is usually pre-processed by pass-band and stop-band filters that can modify some features of the EEG signals and that are essentially linear filters. However, given the nature of these signals, adaptive filters that can preserve their nonlinear information will be more adequate to analyze them. The nature of EEG signals naturally harmonizes with the use of EMD and Hilbert Huang Transform (HHT) to obtain a better signal representation and to detect instantaneous frequencies that with other methods are difficult to observe [5]. The nonlinear parameters will then better describe the dynamics of the EEG signals considering their nonlinear and non-stationary nature [6].

In [7], a method to quantify interaction between nonstationary cerebral blood velocity (BFV) and blood pressure (BP) is proposed for the assessment of dynamic cerebral autoregulation (CA) using HHT. In [8] the authors show a novel feature extraction methodology for the classification of EEG signals involving the calculation of EMD. A bandwidth parameter, measured from the analytic signal representation of IMFs obtained from the EMD method, for classification of seizure and nonseizure EEG signals is presented in [9]. In [10], the authors show an evolution of EMD called Multivariate Empirical Mode Decomposition (MEMD), which is very useful in direct multichannel data analysis; in that case used for a full data-driven analysis to decompose resting-state fMRI (functional Magnetic Resonance Imaging) data into different sub-bands looking for connectivity functions. This paper has a similar purpose, but instead of using fMRI we use EEG signals and another brain reconstruction algorithm, in this case we used IRA-L2 (Iterative Regularization Algorithm with norm $l-2$). The use of fMRI implies higher costs and low accessibility due to the equipment required for acquisition and processing of information.

Different strategies have been used for the process of reconstruction of Neural Activity from EEG data, but the use of EMD has been scarcely reported and its performance is still an open issue due to the challenge posed in the selection of relevant modes for activity reconstruction [5], [11], [12], [13]. One of the alternatives is to apply the methodology of the inverse problem. An iterative regularized method that explicitly includes space (grounded in a physiological model) and time constraints within the dynamic solution of the EEG inverse problem is presented in [14].

The treatment of focal epilepsy when the medicines to control epileptic seizures are not effective, consists in a surgery where a part of the brain is removed. The surgery is performed after carefully locating the sources or brain zones that initiate the epileptic seizures. The smaller the region that is removed, the lower the effects on the patient will be. Therefore, highly precise brain mapping techniques are required to performed this task. However, when precise mapping is not available, an additional surgery is performed in order to obtain additional estimation of the zone that has to be removed by using intra-cranial electrodes [15]. Multiple studies have been done on the detection of the risk of epilepsy. For example, in [16], the authors presented a comparison between the performance of a Genetic Algorithm (GA) and Multi- Layer Perceptron (MLP) Neural network in the classification of epilepsy risk

Manuscript received July 31, 2018; revised January 11, 2019. This work was carried out under the funding of the Departamento Administrativo Nacional de Ciencia, Tecnología e Innovación (Colciencias). Research project: 111077757982 “Sistema de identificación de fuentes epileptogénicas basado en medidas de conectividad funcional usando registros electroencefalográficos e imágenes de resonancia magnética en pacientes con epilepsia refractaria: apoyo a la cirugía resectiva”.

M. Bueno-López is with the Department of Electrical Engineering, Universidad de La Salle, Bogotá, Colombia, e-mail: maxbueno@unisalle.edu.co.

P.A. Munoz-Gutierrez is with the Department of Electronic Engineering, Universidad del Quindío, Armenia, Colombia, e-mail: pamunoz@uniquindio.edu.co.

E. Giraldo is with the Department of Electrical Engineering, Universidad Tecnológica de Pereira, Pereira, Colombia, e-mail: egiraldos@utp.edu.co.

M. Molinas is with the Department of Engineering Cybernetics, Norwegian University of Science and Technology, Trondheim, Norway, e-mail: marta.molinas@ntnu.no

level from EEG signal parameters. The epilepsy risk level is classified based on the extracted parameters like energy, variance, peaks, sharp and spike waves, duration, events and covariance from the EEG of the patient. In [17], the authors show the application of Multi-Layer Perceptron (MLP) as an optimizer for classification of epilepsy risk levels obtained from the fuzzy techniques using EEG signal parameters. The obtained risk level patterns from fuzzy techniques are found to have low values of Performance Index (PI). Another good approximation in this topic has been presented in [18]. In that paper is intended to compare the performance of four different types of fuzzy aggregation methods in classification of epilepsy risk levels from EEG Signal parameters.

In this paper, an improvement is proposed for a brain mapping technique by introducing a pre-processing stage of the EEG signals. The main goal is to develop a more precise brain mapping method that classifies the information into frequency bands from the IMFs. In this way, it will be possible to more precisely locate the area in the brain where the epileptic seizures occur. To this end, an automatic selection of IMFs is performed based on an entropy cost function. The entropy is an indicator of the amount of information stored in a more general probability distribution and is a measure of the complexity of the time series [19]. As a result an Enhanced Empirical Mode Decomposition is obtained for EEG -based activity source reconstruction. Some previous works have considered the use of entropy to detect the source of epileptic seizure [20], [21]. We applied EMD in simulated and real EEG signals containing normal and epileptic activity based on a nonlinear complex model. The simulated EEG signals are generated for one active source under several noise conditions. In order to detect the sources associated to epileptic seizures a brain mapping stage is performed using a reconstructed EEG signals obtained from the optimally selected IMFs. A relative error measure is used to compare the brain mapping results from the EEG database without applying EMD and the optimally reconstructed signals using EMD. An additional evaluation over real EEG signals containing epileptic seizures events is performed.
The paper is organized as follows: Section II gives an introduction to the essential concepts of EMD and EEG signals. The experimental setup is presented in Section III and the results obtained with the EEG signals are presented in Section IV. The discussion of the results is presented in Section V. Finally, some conclusions are given in Section VI.

II. Materials and Methods

A. Brain Mapping: The Inverse Problem

The forward problem of EEG generation can be formulated

$$\boldsymbol{y}(t_k) = \boldsymbol{M}\boldsymbol{x}(t_k) + \boldsymbol{\epsilon}(t_k) \tag{1}$$

being $\boldsymbol{y}(t_k) \in \mathbb{R}^d$ the EEG, and $\boldsymbol{x}(t_k) \in \mathbb{R}^n$ the neural activity, with $t_k = kh$ the time at sample k being $k = 1, \ldots, T$ the total number of samples, h the sample time and $\boldsymbol{M} \in \mathbb{R}^{d \times n}$ the lead-field matrix that relates the neural activity with the EEG. The evolution of $\boldsymbol{x}(t_k)$ in time can be used to model several behaviors of the EEG signals. It is possible to formulate an iterative inverse problem (IRA-L2) [14] in order to estimate the neural activity $\widehat{\boldsymbol{x}}(t_k)$ for each measurement $\boldsymbol{y}(t_k)$, as described in:

$$\begin{aligned}\widehat{\boldsymbol{x}}(t_k) = \arg\min_{\boldsymbol{x}(t_k)} \|\boldsymbol{y}(t_k) - \boldsymbol{M}\boldsymbol{x}(t_k)\|_2^2 + \alpha_k \|\boldsymbol{x}(t_k)\|_1 \\ + \lambda_k \|\boldsymbol{x}(t_k) - \widehat{\boldsymbol{x}}(t_{k-1})\|_2^2\end{aligned} \tag{2}$$

being λ_k and α_k the regularization parameters computed by generalized cross validation [14].

B. Empirical Mode Decomposition

The Empirical Mode Decomposition (EMD) is an adaptive, and data-dependent method. The aim of the EMD method is to decompose the nonlinear and non-stationary signal $\boldsymbol{y}(t_k)$ into a sum of intrinsic mode functions (IMFs) that satisfies two conditions [22]:

1) The number of extrema and the number of zero crossings must be the same or differ at most by one.
2) At any point, the mean value of the envelope defined by the local maxima and the envelope defined by the local minima is zero.

The EMD algorithm can be summarized in Fig. 1

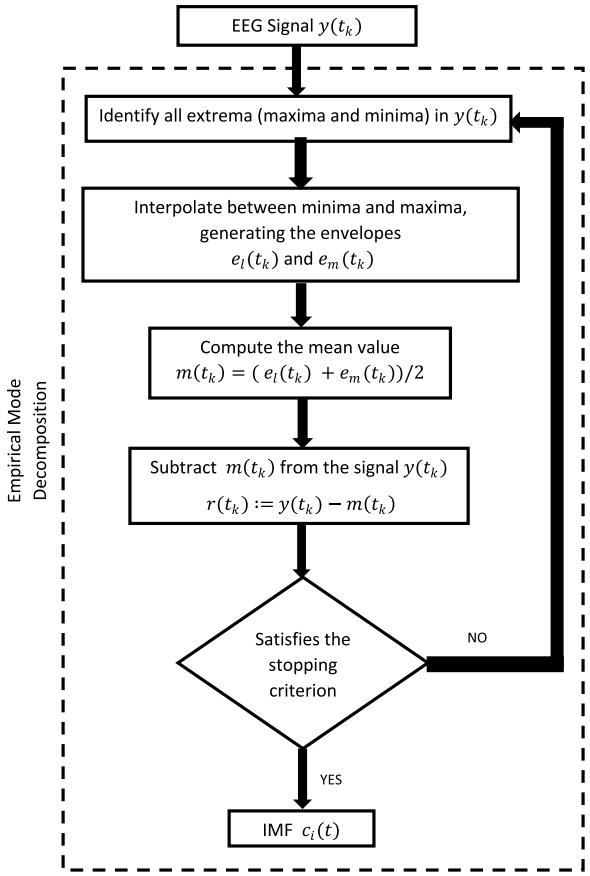

Fig. 1. Flowchart indicating the various stages of the EMD method

Empirical Mode Decomposition is applied over $\boldsymbol{y}(t_k)$ to obtain $\boldsymbol{\gamma}_i(t_k)$ being i the intrinsic mode function (IMF), and

$$\boldsymbol{y}(t_k) = \sum_{i=1}^{N} \boldsymbol{\gamma}_i(t_k) + \boldsymbol{r}(t_k) \tag{3}$$

where N is the number of IMFs and $\boldsymbol{r}(t_k)$ a residual. Recently, some optimization techniques have been proposed to improve the performance of the EMD [23], [24].

Having obtained the intrinsic mode function components, we can apply the Hilbert transform to each IMF component, and compute the instantaneous frequency according to equation (4).

$$f_i(t) \triangleq \frac{1}{2\pi} \cdot \frac{d\theta_i(t)}{dt}, \tag{4}$$

where $\theta_i(t)$ is the function phase of each IMF calculated from the analytic signal associated [25]. Finally, the instantaneous frequency can be observed in the Hilbert Spectrum.

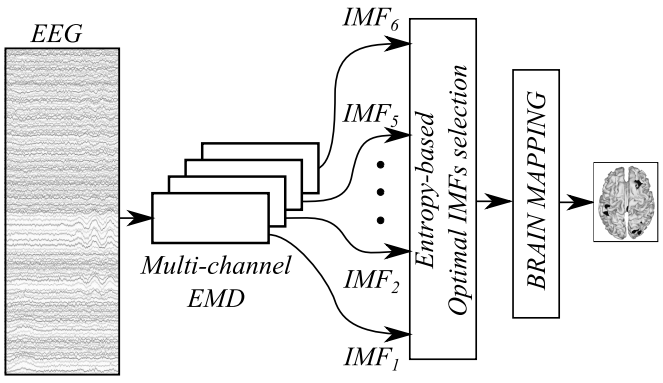

Fig. 2. Experimental setup for entropy-based selection of IMFs

C. Automatic IMF selection: Entropy Function

An entropy based cost function is applied over each IMF $\boldsymbol{\gamma}_i(t_k)$ as follows:

$$e_i = -\sum_k \|\boldsymbol{\gamma}_i(t_k)\|_2^2 \log(\|\boldsymbol{\gamma}_i(t_k)\|_2^2) \tag{5}$$

being e_i the entropy of each IMF, and $\boldsymbol{e} = [e_1 \dots e_N]$. In order to reconstruct the EEG signal $\tilde{\boldsymbol{y}}(t_k)$ an automati selection of the IMFs (IMFs with highest entropy) are applied according to the measured entropy e_i.

$$\tilde{\boldsymbol{y}}(t_k) = \sum_{i \in O} \boldsymbol{\gamma}_i(t_k) \tag{6}$$

being O the subset of of IMFs whose entropy e_i is over a threshold τ_e computed as follows

$$\tau_e = \frac{\max \boldsymbol{e} - \min \boldsymbol{e}}{2} + \min \boldsymbol{e} \tag{7}$$

III. Experimental setup

The performance of the aforementioned method is evaluated by using simulated and real EEG signals containing epileptic seizures. The experimental setup is divided in the following tasks, as depicted in Fig. 2:

1) EEG acquisition or simulation $\boldsymbol{y}(t_k)$.
2) Apply EMD on the EEG signal.
3) Optimal selection of IMFs using an entropy based cost function.
4) Reconstruction of a signal $\tilde{\boldsymbol{y}}(t_k)$ based on the optimally selected IMFs according to (7).
5) Brain mapping of the neural activity based on the reconstructed signal.
6) Detection of focal origin of Epileptic seizures is performed by locating the source where the seizure is generated.

Four methods are considered for brain mapping comparison to evaluate the performance of the proposed algorithm:

1) Brain mapping ($\widehat{\boldsymbol{x}}(t_k)$) using the EEG database $\boldsymbol{y}(t_k)$ without EMD.
2) Brain mapping ($\widehat{\boldsymbol{x}}_{\boldsymbol{EMD}}(t_k)$) using the reconstructed EEG $\tilde{\boldsymbol{y}}(t_k)$ obtained from EMD standard decomposition and an entropy based IMF selection.
3) Brain mapping ($\widehat{\boldsymbol{x}}_{\boldsymbol{W}}(t_k)$) using the reconstructed EEG $\tilde{\boldsymbol{y}}_{\boldsymbol{W}}(t_k)$ obtained from Wavelet Transform using Daubechies wavelet and three decompositions levels, where the level with highest energy is selected for reconstruction of the EEG.
4) Brain mapping ($\widehat{\boldsymbol{x}}_{\boldsymbol{WP}}(t_k)$) using the reconstructed EEG $\tilde{\boldsymbol{y}}_{\boldsymbol{WP}}(t_k)$ obtained from Wavelet Packets decomposition using Daubechies wavelet and three decompositions levels, where the level with highest entropy is selected for reconstruction of the EEG.

A common procedure to evaluate the performance of brain mapping techniques is by using simulated EEG signals where the underlying brain activity is known. In this case, a measure of the brain mapping quality can be evaluated with the relative error measure [26] as follows:

$$e_s = \sum_k \frac{\|\widehat{\boldsymbol{x}}(t_k) - \boldsymbol{x}(t_k)\|_2^2}{\|\boldsymbol{x}(t_k)\|_2^2} \tag{8}$$

$$e_{EMD} = \sum_k \frac{\|\tilde{\boldsymbol{x}}_{\boldsymbol{EMD}}(t_k) - \boldsymbol{x}(t_k)\|_2^2}{\|\boldsymbol{x}(t_k)\|_2^2} \tag{9}$$

$$e_W = \sum_k \frac{\|\tilde{\boldsymbol{x}}_{\boldsymbol{W}}(t_k) - \boldsymbol{x}(t_k)\|_2^2}{\|\boldsymbol{x}(t_k)\|_2^2} \tag{10}$$

$$e_{WP} = \sum_k \frac{\|\tilde{\boldsymbol{x}}_{\boldsymbol{WP}}(t_k) - \boldsymbol{x}(t_k)\|_2^2}{\|\boldsymbol{x}(t_k)\|_2^2} \tag{11}$$

being e_s the reconstruction error of the brain mapping estimation $\widehat{\boldsymbol{x}}(t_k)$ resulting from $\boldsymbol{y}(t_k)$, e_{EMD} the reconstruction error of the brain mapping estimation $\tilde{\boldsymbol{x}}_{\boldsymbol{EMD}}(t_k)$ resulting from $\boldsymbol{y}(t_k)$, e_W the reconstruction error of the brain mapping estimation $\tilde{\boldsymbol{x}}_{\boldsymbol{W}}(t_k)$ resulting from $\tilde{\boldsymbol{y}}_{\boldsymbol{W}}(t_k)$ and e_{WP} the reconstruction error of the brain mapping estimation $\tilde{\boldsymbol{x}}_{\boldsymbol{WP}}(t_k)$ resulting from $\tilde{\boldsymbol{y}}_{\boldsymbol{WP}}(t_k)$.

A. Simulated EEG signals

For the first simulated database (SD-1) a complex nonlinear model of neural activity is used for EEG generation during an epileptic seizure based on [27] as follows

$$\begin{aligned}\boldsymbol{x}(t_k) = {} & \boldsymbol{A}_1\boldsymbol{x}(t_{k-1}) + \boldsymbol{A}_2\boldsymbol{x}(t_{k-2}) \\ & + \boldsymbol{A}_3\boldsymbol{x}(t_{k-\tau}) + \boldsymbol{A}_4\boldsymbol{x}(t_{k-1})^{\circ 2} + \boldsymbol{A}_5\boldsymbol{x}(t_{k-1})^{\circ 3} + \boldsymbol{\eta}(t_k)\end{aligned} \tag{12}$$

being $\boldsymbol{A}_1 = a_1\boldsymbol{I}_n$, $\boldsymbol{A}_2 = a_2\boldsymbol{I}_n$, $\boldsymbol{A}_3 = a_3\boldsymbol{I}_n$, $\boldsymbol{A}_4 = a_4\boldsymbol{I}_n$ and $\boldsymbol{A}_5 = a_5\boldsymbol{I}_n$, where $\boldsymbol{I}_n \in \mathbb{R}^{n\times n}$ is an identity matrix and $a_i \in \mathbb{R}$, are the model parameters which describe the dynamics of the brain activity, where $\boldsymbol{c}_{k-1}^{\circ 2}$ denotes the Hadamard Power. The model parameter are set to $\tau = 20$, $a_1 = 1.0628$, $a_2 = -0.42857$, $a_3 = 0.008$, $a_4 = 0.000143$, $a_5 = -0.000286$,

and $\|\boldsymbol{\eta}(t_k)\| \leq 0.05$. The epileptic seizure is simulated at time $t_k = 0.5\,s$ by modifying the values of a_1 from 1.0628 to 1.3, while a_2 from -0.428 to -1 over the entire diagonal. The simulated EEG $\boldsymbol{y}(t_k)$ is obtained from $\boldsymbol{x}(t_k)$ using (1) where $\boldsymbol{\epsilon}(t_k)$ is set to achieve the Signal-to-Noise Ratios (SNRs) of 0, 5, 10, 15 and 20 *dB*, the sample rate is 250Hz, and a number of $d = 128$ electrodes and $n = 8196$ sources are considered.

For the second simulated database (SD-2), the epileptic seizure is simulated at time $t_k = 0.5\,s$ by using a sinusoidal signal with frequencies linearly varying in the range of 8 to 12Hz [14]. The simulated EEG $\boldsymbol{y}(t_k)$ is obtained from $\boldsymbol{x}(t_k)$ using (1) where $\boldsymbol{\epsilon}(t_k)$ is set to achieve the Signal-to-Noise Ratios (SNRs) of 0, 5, 10, 15 and 20 *dB*. The sample rate is 500Hz, and a number of $d = 128$ electrodes and $n = 8196$ sources are considered.

B. Real EEG signals

The real EEG database (RD) is recorded from two patients one having frontal and another temporal lobe epilepsy [14]. Data were collected during routine clinical practice (Instituto de Epilepsia y Parkinson del Eje Cafetero from Pereira, Colombia), in an awake resting state. All patients signed the informed consent form before being enrolled into the study, and the process was approved by the ethical committee. A number of $d = 34$ electrodes are placed according to the $10-20$ system and data is sampled at rate of 1kHz with 16 bits-resolution. For the purpose of analysis, each 1 s time series is segmented from the long recording around the beginning of the ictal event, that is at $t = 0.5$ s. It is worth noting that the pre-processing stage to remove noise or artifacts is not considered for the real EEG recordings. The testing head structure assumes $n = 20484$, where all sources are placed on the tessellated cortex surface and are perpendicular to it. For the real database, an additional analysis of epileptic seizure detection is performed based on the Hilbert spectrum.

IV. Results

A. Simulated Data Base

An example of the EEG signal for SD-1 for a SNR of 0 *dB* is shown in Fig. 3. The analyzed signals are nonlinear and nonstationary, therefore the EMD is a good alternative to obtain information. An example of the signal in one channel is presented in Fig. 4.

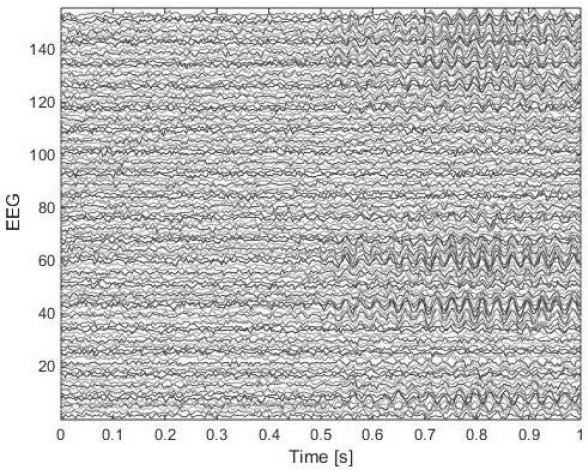

Fig. 3. Simulated EEG for SD-1

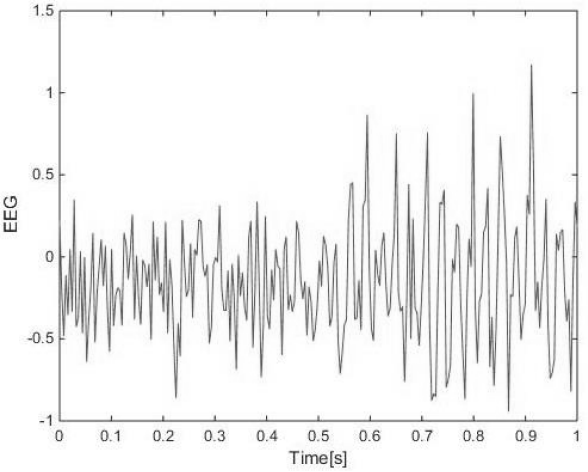

Fig. 4. Example of one channel of simulated EEG for SD-1

After analyzing the database with the EMD, we obtained 6 IMFs per channel. In the IMF 2 in Fig. 5, it is possible to observe two areas in red that show how different frequencies (different oscillations) appear in the same IMF. In these IMFs the mode mixing problem is evident [28]. An example of the retained energy and entropy for each IMF is presented in Fig. 6. In this example, the threshold is $\tau_e = 1930.9$ and then the EEG signal is reconstructed by using the IMF_1 and IMF_2.

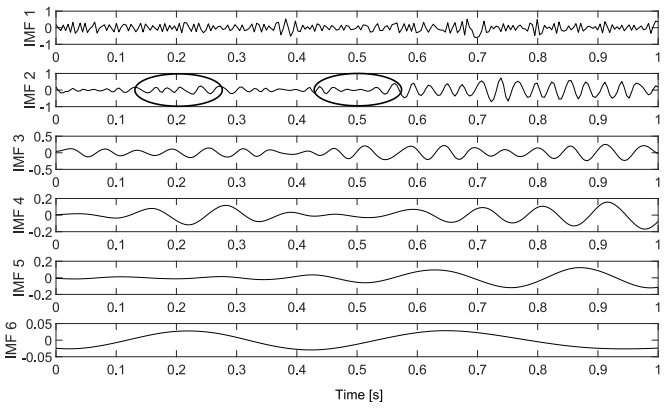

Fig. 5. IMFs of y_s for SD-1 using standard EMD

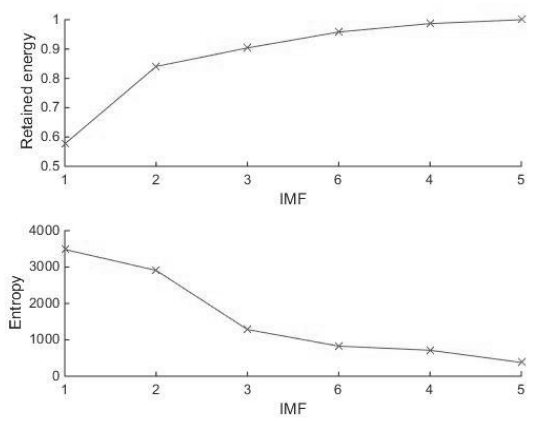

Fig. 6. Retained energy and entropy of $\boldsymbol{y}(t_k)$ for SD-1 using standard EMD

An example of the Hilbert spectrum is presented in Fig. 7, it is possible to see how the instantaneous frequency is changing over time. As expected, it is observed that the highest frequency is in IMF 1 ($c_1(t)$).

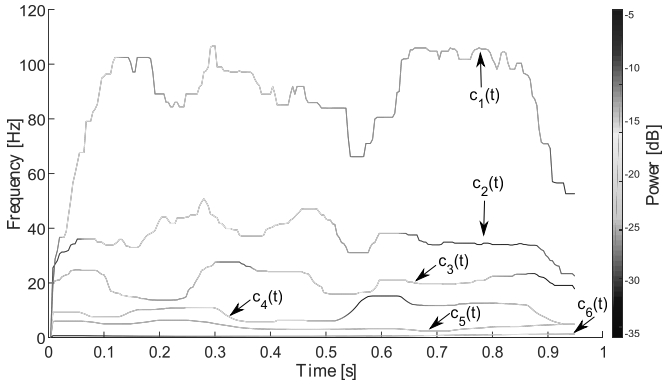

Fig. 7. Hilbert spectrum of $\boldsymbol{y}(t_k)$ for SD-1 using standard EMD

A comparison of the original $\boldsymbol{y}(t_k)$ and reconstructed $\tilde{\boldsymbol{y}}(t_k)$ signals is presented in Fig. 8. The resulting brain mapping for each method is presented in Fig 9.

Relative error measure is used for evaluation. For the above example the relative errors based on (8) are as follows:

$$\begin{aligned} e_s &= 1.3284 \\ e_{EMD} &= 1.2942 \\ e_W &= 1.3106 \\ e_{WP} &= 1.2007 \end{aligned}$$

showing that the best result is obtained for the brain mapping computed from the reconstructed neural activity using entropy-based selection of IMFs. An analysis based on 30 trials for each noise condition is shown in Fig. 10. As shown in Fig. 10, the best results are achieved by the proposed method of EMD decomposition with automatic selection of relevant IMFs based on the entropy measure (EMD-entropy). Therefore, for SD-2 and the Real Database, the comparison is performed only for the EEG data with and without the EMD stage. An example of the signal in one channel is presented in Fig. 11 and the resulting IMFs for SD-2 using standard EMD is presented in Fig. 12.

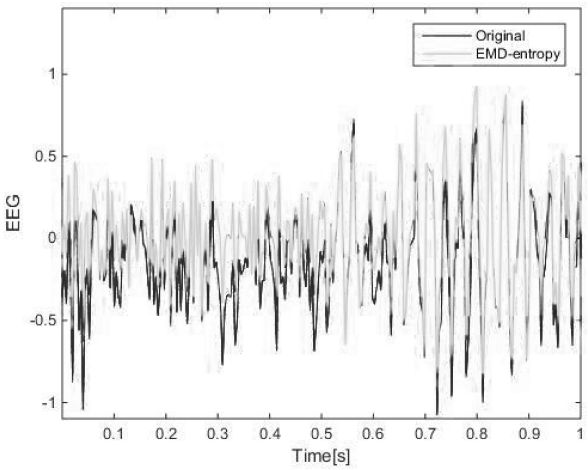

Fig. 8. Comparison of simulated $\boldsymbol{y}(t_k)$ and optimally reconstructed $\tilde{\boldsymbol{y}}(t_k)$ signals for SD-1 by using standard EMD for one channel

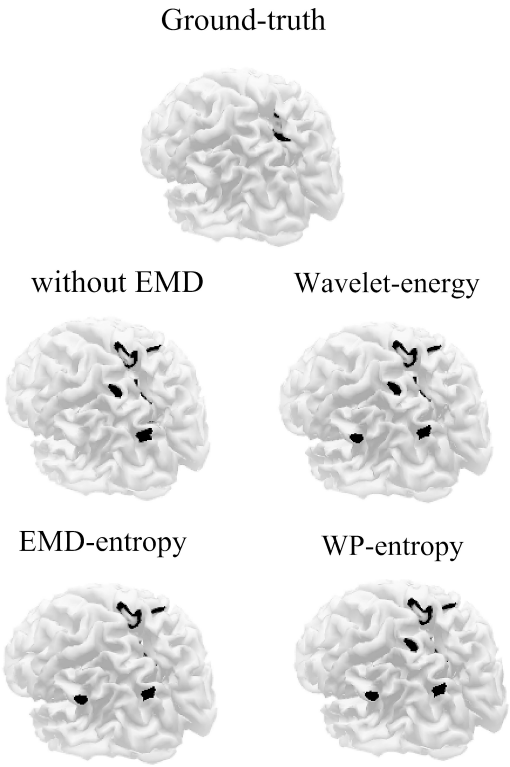

Fig. 9. Comparison of brain mapping obtained for simulated $\boldsymbol{x}(t_k)$, estimated without EMD $\widehat{\boldsymbol{x}}(t_k)$ and optimally reconstructed $\tilde{\boldsymbol{x}}(t_k)$ neural activity for SD-1

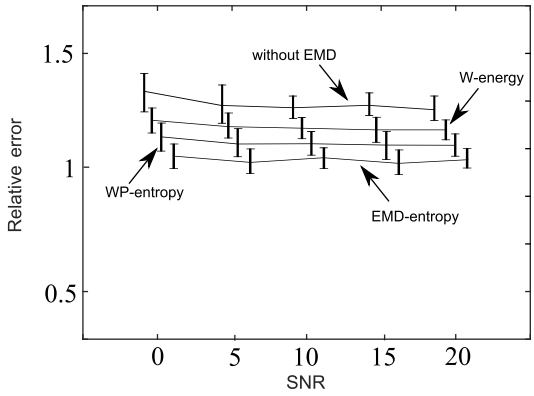

Fig. 10. Relative error comparison for SD-1 under several noise conditions

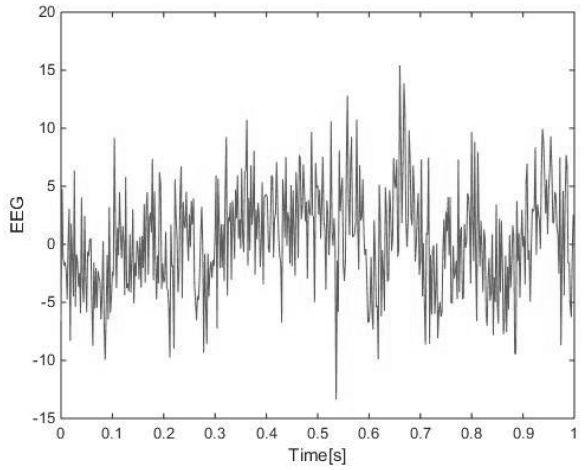

Fig. 11. Example of one channel of simulated EEG for SD-2

The retained energy and entropy for each IMF are presented in Fig. 13. In this example, the threshold is $\tau_e = -1.4239 \times 10^6$ and then the EEG $\tilde{\boldsymbol{y}}(t_k)$ is reconstructed by using the IMF_3, IMF_2, IMF_6 and IMF_5.

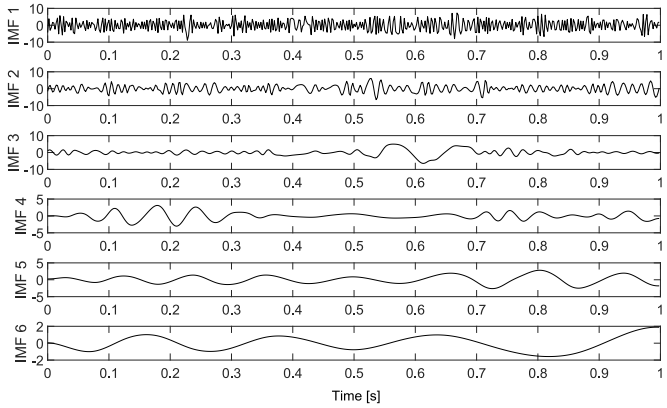

Fig. 12. IMFs of $\boldsymbol{y}(t_k)$ for SD-2 using standard EMD

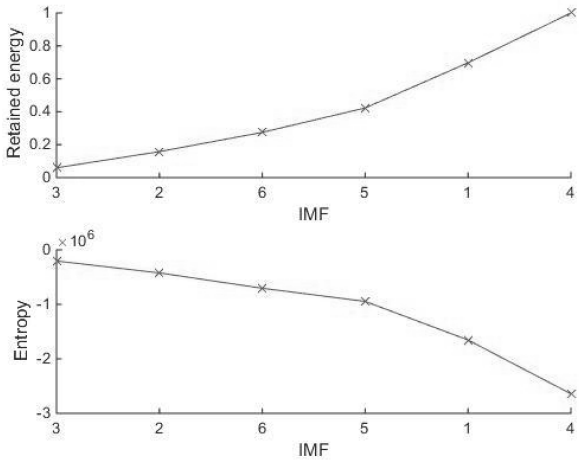

Fig. 13. Retained energy and entropy of $\boldsymbol{y}(t_k)$ for SD-2 using standard EMD

An example of the Hilbert spectrum is presented in Fig. 14 and a comparison of the original and reconstructed signals is shown in Fig. 15. The resulting brain mapping for each method applied in SD-2 is presented in Fig 16. Relative error measure is used for evaluation. For the above example, the relative errors are as follows:

$$e_s = 1.3284$$
$$e_r = 1.2942$$

A comparison in terms of the relative error for 30 trials of the SD-2 is shown in Fig. 17.

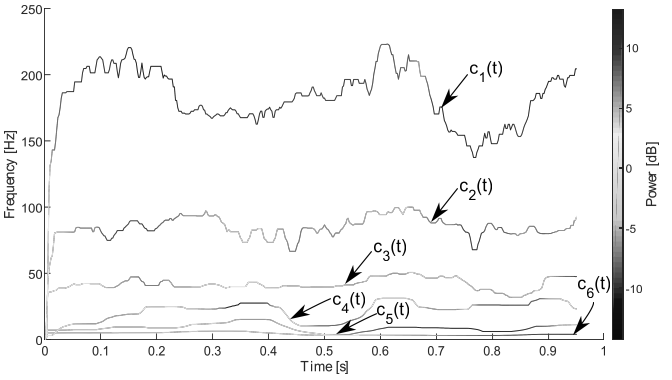

Fig. 14. Hilbert spectrum of $\boldsymbol{y}(t_k)$ for SD-2 using standard EMD

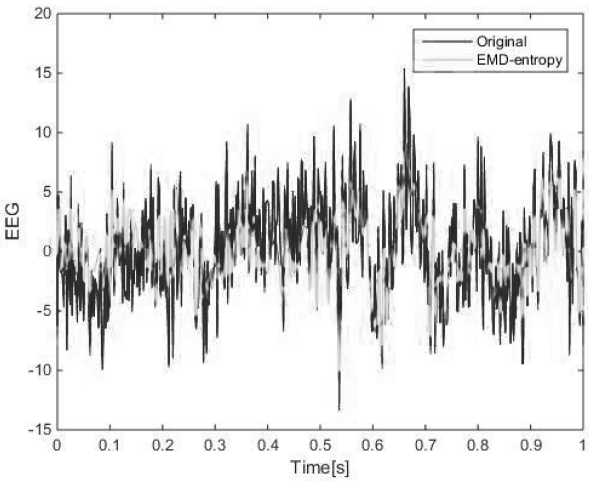

Fig. 15. Comparison of simulated $\boldsymbol{y}(t_k)$ and optimally reconstructed $\tilde{\boldsymbol{y}}(t_k)$ signals for SD-2 by using standard EMD for one channel

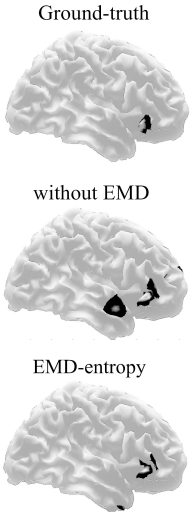

Fig. 16. Comparison of brain mapping obtained for simulated $\boldsymbol{x}(t_k)$, estimated without EMD $\widehat{\boldsymbol{x}}(t_k)$ and optimally reconstructed $\tilde{\boldsymbol{x}}(t_k)$ neural activity for SD-1

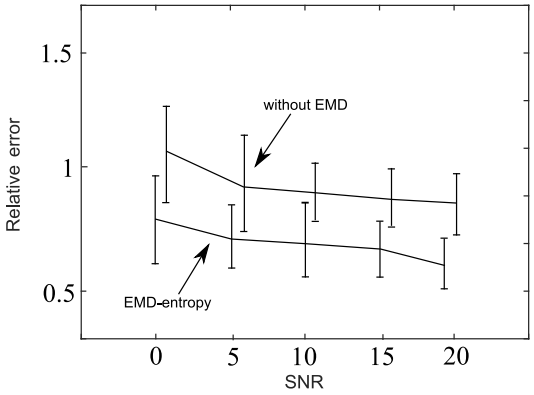

Fig. 17. Comparison of relative error measure in reconstruction for SD-2 under several noise conditions

From the above, it can be seen an improvement of the source localization in terms of the relative error. This improvement is encouraging for further investigation since during epilepsy surgery the brain area where epileptic seizures begin is removed.

B. Real Data Base

An example of the EEG from the RD is presented in 18.

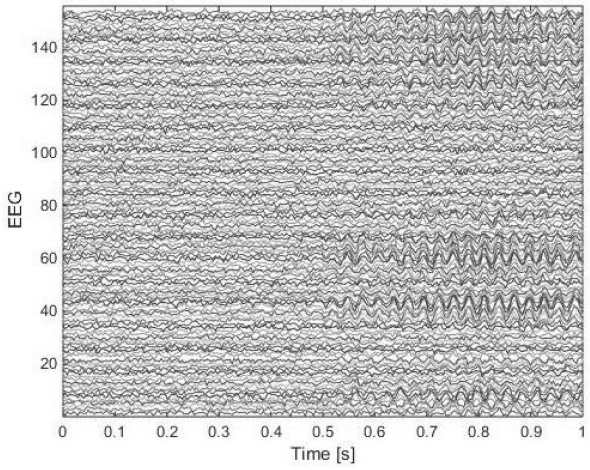

Fig. 18. EEG from RD

For the real database a comparison of the original and reconstructed signal is presented in Fig. 19. The reconstructed signal is the sum of an optimal selection of the IMFs 4, 3 and 5.

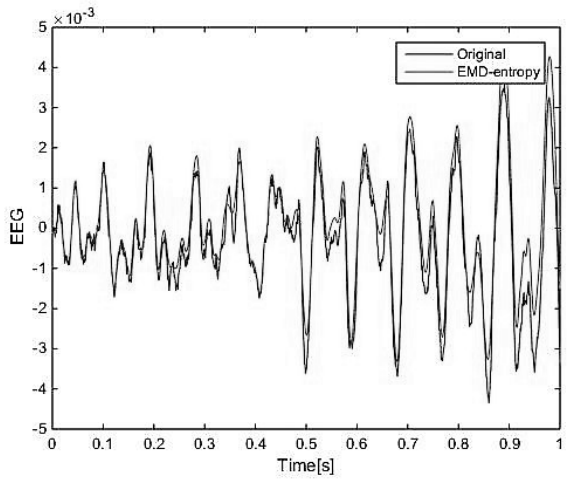

Fig. 19. Comparison of real EEG signal and optimally reconstructed signal by using standard EMD for one channel

The resulting IMFs using standard EMD are presented in Fig. 20

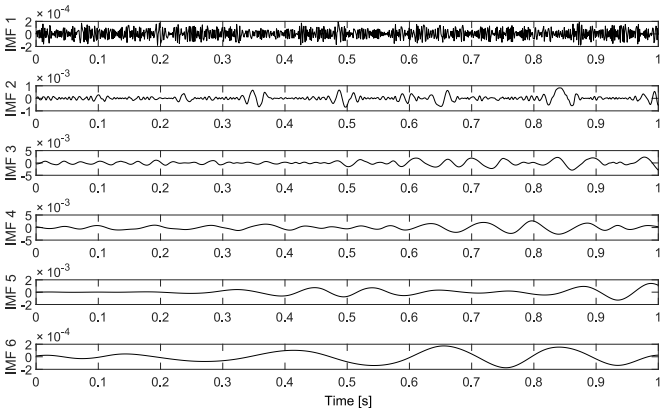

Fig. 20. IMFs of real database using standard EMD

An example of the retained energy and entropy for each IMF is presented in Fig. 21. It can be seen that the IMFs are ordered according to the entropy values. In this case, the IMFs 4, 3 and 5 are used to reconstruct the signal since they are over the defined entropy threshold. An example of the frequency spectrum using Hilbert is presented in Fig. 22. The resulting brain mapping for each method is presented in Fig 23.

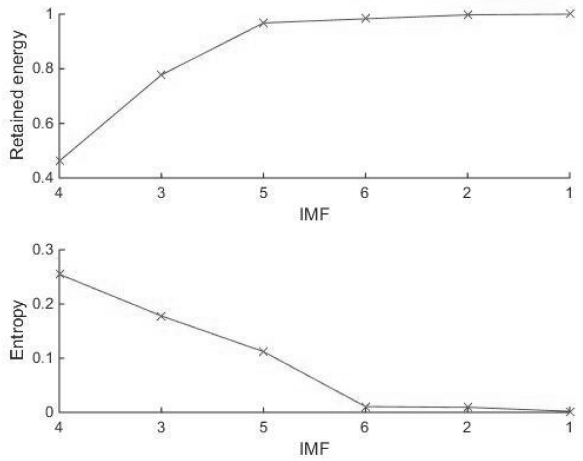

Fig. 21. Retained energy and entropy of real database using standard EMD

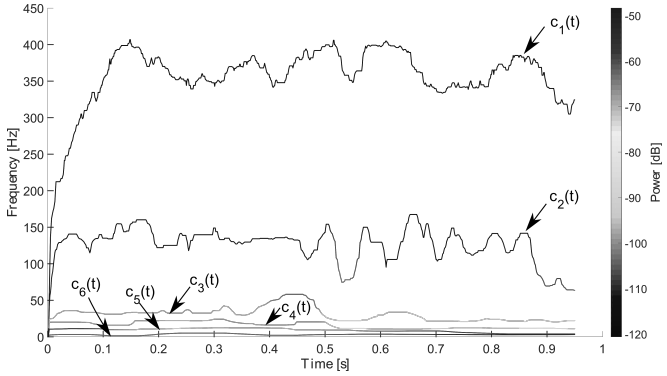

Fig. 22. Hilbert spectrum of real database using standard EMD

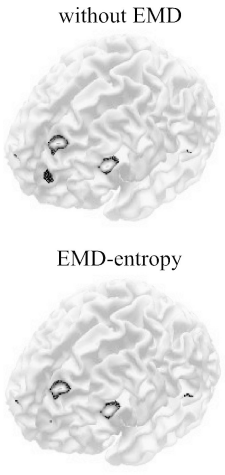

Fig. 23. Comparison of brain mapping obtained for real database $\widehat{\boldsymbol{x}}(t_k)$ and optimal reconstructed $\tilde{\boldsymbol{x}}(t_k)$ neural activity

V. Discussion

In this section we highlight some aspects that allow us to show the usefulness of the methodology proposed. The decomposition using IMFs allows us to reconstruct the neuronal activity using only the information that is considered relevant for this application. According to some previous works [5], the EMD does not have a good performance in decomposing and reconstructing the signals with low frequency because of the problem of mode mixing. In Figures 5, 12 and 20 is possible to observe this phenomena. Some methodologies such as the masking signal [29] or Ensamble Empirical Mode Decomposition (EEMD) have been proposed to avoid this problem [30]. The mode mixing does not disappear completely, however the technique is very interesting when it is compared with other strategies quite common for this type of application, for example with Discrete Wavelet Transform (DWT) is necessary to consider four factors affecting the performance in epileptic focus localization: the mother wavelet, the level of decomposition, frequency bands, and features [31]. Based on the above, we have proposed a new and simple methodology based on an entropy function that allows us to select the IMFs regardless of the mode mixing problem. The threshold value proposed in (7) was obtained after several tests with the values of entropy and retained energy in each IMF. The first validation using simulated databases allowed us to calculate the relative error and to affirm that the technique presented provides an accurate detection of sources associated to epileptic seizures. In Figures 9 and 16 is possible to observe the desired mapping (ground-truth) and the values obtained without EMD and with the proposed method (EMD-entropy). In both cases, the relative error is lower with our method. In the first case, the EEG is reconstructed by using the IMF_1 and IMF_2 and in the second case we used the IMF_3, IMF_2, IMF_6 and IMF_5. The IMFs are selected automatically, and depending of the EEG the number of IMFs could change, but in either case the sources are located exactly. In both cases, the epileptic seizure appears at time $t_k = 0.5s$ and although time localization was not one of the purposes of this paper, it can be observed in the Hilbert spectrum that the instantaneous frequencies associated with each IMF have a change in their behavior at exactly this time, therefore an additional analysis of the instantaneous frequency could be performed in order to automatically detect the onset of an epileptic activity.

VI. Conclusions

In this work, we presented a technique for automatic detection of sources associated to epileptic seizures based on EMD and an entropy function. This strategy avoids the use of common methods that need expert clinicians visual inspection of electroencephalography (EEG) signals, which tends to be time consuming and sensitive to bias. The tests carried out with the simulated databases and real databases and the calculation of the relative error measure show an promising performance of the proposed methodology.

References

[1] C. Im and J.-M. Seo, "A review of electrodes for the electrical brain signal recording," *Biomedical Engineering Letters*, vol. 6, no. 3, pp. 104–112, Aug 2016.

[2] D. P. Subha, P. K. Joseph, R. Acharya U, and C. M. Lim, "EEG signal analysis: A survey," *Journal of Medical Systems*, vol. 34, no. 2, pp. 195–212, Apr 2010.

[3] M. Soleymani, S. Asghari-Esfeden, Y. Fu, and M. Pantic, "Analysis of EEG signals and facial expressions for continuous emotion detection," *IEEE Transactions on Affective Computing*, vol. 7, no. 1, pp. 17–28, Jan 2016.

[4] K. Y. Lin, D. Y. Chen, and W. J. Tsai, "Face-based heart rate signal decomposition and evaluation using multiple linear regression," *IEEE Sensors Journal*, vol. 16, no. 5, pp. 1351–1360, March 2016.

[5] M. Bueno-Lopez, E. Giraldo, and M. Molinas, "Analysis of neural activity from EEG data based on emd frequency bands," in *24th IEEE International Conference on Electronics, Circuits and Systems (ICECS)*, vol. 1. Batumi, Georgia: IEEE, December 2017, pp. 1–5.

[6] R. Sharma, R. B. Pachori, and U. R. Acharya, "Application of entropy measures on intrinsic mode functions for the automated identification of focal electroencephalogram signals," *Entropy*, vol. 17, pp. 669–691, 2015.

[7] L. Men-Tzung, H. Kun, L. Yanhui, C. Peng, and N. Vera, "Multimodal pressure-flow analysis: Application of hilbert huang transform in cerebral blood flow regulation," *EURASIP Journal on Advances in Signal Processing*, vol. 2008, no. 1, pp. 1–15, May 2008.

[8] F. Riaz, A. Hassan, S. Rehman, I. K. Niazi, and K. Dremstrup, "EMD-based temporal and spectral features for the classification of EEG signals using supervised learning," *IEEE Transactions on Neural Systems and Rehabilitation Engineering*, vol. 24, no. 1, pp. 28–35, Jan 2016.

[9] V. Bajaj and R. B. Pachori, "Classification of seizure and nonseizure eeg signals using empirical mode decomposition," *IEEE Transactions on Information Technology in Biomedicine*, vol. 16, no. 6, pp. 1135–1142, Nov 2012.

[10] T. Zhang, P. Xu, L. Guo, R. Chen, R. Zhang, H. He, Q. Xie, T. Liu, C. Luo, and D. Yao, "Multivariate empirical mode decomposition based sub-frequency bands analysis of the default mode network: a resting-state fmri data study," *Applied Informatics*, vol. 2, no. 1, p. 2, Jan 2015.

[11] A. Zahra, N. Kanwal, N. Rehman, S. Ehsan, and K. D. McDonald-Maier, "Seizure detection from EEG signals using multivariate empirical mode decomposition," *Computers in Biology and Medicine*, vol. 88, no. July, pp. 132–141, 2017.

[12] P. Munoz-Gutiérrez, E. Giraldo, M. Bueno-López, and M. Molinas, "Localization of active brain sources from EEG signals using empirical mode decomposition: A comparative study," *Frontiers in Integrative Neuroscience*, vol. 12, no. 1, pp. 1–13, 2018.

[13] M. Bueno-López, P. A. Muñoz-Gutiérrez, E. Giraldo, and M. Molinas, "Analysis of epileptic activity based on brain mapping of eeg adaptive time-frequency decomposition," in *Brain Informatics*, S. Wang, V. Yamamoto, J. Su, Y. Yang, E. Jones, L. Iasemidis, and T. Mitchell, Eds. Cham: Springer International Publishing, 2018, pp. 319–328.

[14] E. Giraldo-Suarez, J. Martinez-Vargas, and G. Castellanos-Dominguez, "Reconstruction of neural activity from eeg data using dynamic spatiotemporal constraints," *International Journal of Neural Systems*, vol. 26, no. 07, pp. 1–15, 2016.

[15] C. Plummer, A. S. Harvey, and M. Cook, "Eeg source localization in focal epilepsy: Where are we now?" *Epilepsia*, vol. 49, no. 2, pp. 201–218, 2008. [Online]. Available: http://dx.doi.org/10.1111/j.1528-1167.2007.01381.x

[16] R. Sukanesh and R. Harikumar, "A comparison of genetic algorithm & neural network (MLP) in patient specific classification of epilepsy risk levels from EEG signals," *Engineering Letters*, vol. 14, no. 1, pp. 96–104, 2007.

[17] ——, "A patient specific neural networks (MLP) for optimization of fuzzy outputs in classification of epilepsy risk levels from EEG signals," *Engineering Letters*, vol. 13, no. 2, pp. 50–56, 2006.

[24] T. Y. Hou and Z. Shi, "Data-driven time-frequency analysis," *Applied and Computational Harmonic Analysis*, vol. 35, no. 2, pp. 284–308, Sept 2013.

[18] ——, "Diagnosis and classification of epilepsy risk levels from eeg signals using fuzzy aggregation techniques," *Engineering Letters*, vol. 14, no. 1, pp. 90–95, 2007.

[19] M. Costa, A. L. Goldberger, and C.-K. Peng, "Multiscale entropy analysis of complex physiologic time series," *Phys. Rev. Lett.*, vol. 89, p. 068102, Jul 2002. [Online]. Available: https://link.aps.org/doi/10.1103/PhysRevLett.89.068102

[20] J. Xiang, C. Li, H. Li, R. Cao, B. Wang, X. Han, and J. Chen, "The detection of epileptic seizure signals based on fuzzy entropy," *Journal of Neuroscience Methods*, vol. 243, no. Supplement C, pp. 18 – 25, 2015.

[21] L. Wang, W. Xue, Y. Li, M. Luo, J. Huang, W. Cui, and C. Huang, "Automatic epileptic seizure detection in eeg signals using multi-domain feature extraction and nonlinear analysis," *Entropy*, vol. 19, no. 6, pp. 3 – 17, 2017.

[22] N. E. Huang, Z. Shen, S. R. Long, M. C. Wu, H. H. Shih, Q. Zheng, N.-C. Yen, C. C. Tung, and H. H. Liu, "The empirical mode decomposition and the hilbert spectrum for nonlinear and non-stationary time series analysis," *Proceedings of the Royal Society of London A: Mathematical, Physical and Engineering Sciences*, vol. 454, no. 1971, pp. 903–995, 1998.

[23] D. Xu, Y. Xia, and D. P. Mandic, "Optimization in quaternion dynamic systems: Gradient, hessian, and learning algorithms," *IEEE Transactions on Neural Networks and Learning Systems*, vol. 27, no. 2, pp. 249–261, Feb 2016.

[25] B. Boashash, "Estimating and interpreting the instantaneous frequency of a signal. Part 1: Fundamentals," *Proceedings of the IEEE*, vol. 80, no. 4, pp. 520–538, Apr 1992.

[26] R. Grech, T. Cassar, J. Muscat, K. P. Camilleri, S. G. Fabri, M. Zervakis, P. Xanthopoulos, V. Sakkalis, and B. Vanrumste, "Review on solving the inverse problem in eeg source analysis," *Journal of NeuroEngineering and Rehabilitation*, vol. 5, no. 1, p. 25, Nov 2008. [Online]. Available: https://doi.org/10.1186/1743-0003-5-25

[27] P. Munoz and E. Giraldo, "Time-course reconstruction of neural activity for multiples simultaneous source," in *IFMBE Proceedings CLAIB 2016*, vol. 60. Bucaramanga, Colombia: Springer, October 2016, pp. iv/485–iv/488.

[28] G. Rilling and P. Flandrin, "One or two frequencies? The empirical mode decomposition answers," *IEEE Transactions on Signal Processing*, vol. 56, no. 1, pp. 85–95, Jan 2008.

[29] R. Deering and J. F. Kaiser, "The use of a masking signal to improve empirical mode decomposition," in *Proceedings. (ICASSP '05). IEEE International Conference on Acoustics, Speech, and Signal Processing, 2005.*, vol. 4, March 2005, pp. iv/485–iv/488.

[30] Z. Wu and N. E. Huang, "Ensemble Empirical Mode Decomposition: A noise-assisted data analysis method," *Advances in Adaptive Data Analysis*, vol. 1, no. 1, pp. 1–41, 2009.

[31] D. Chen, S. Wan, and F. S. Bao, "Epileptic focus localization using discrete wavelet transform based on interictal intracranial eeg," *IEEE Transactions on Neural Systems and Rehabilitation Engineering*, vol. 25, no. 5, pp. 413–425, May 2017.